Digital Signal Processing ••• (••••) •••–•••

Contents lists available at ScienceDirect

Digital Signal Processing

www.elsevier.com/locate/dsp

Control theoretic approach to tracking radar: First step towards cognition

Simon Haykin *, Amin Zia, Yanbo Xue, Ienkaran Arasaratnam

Cognitive Systems Laboratory, McMaster University, Hamilton, Ontario, L8S 4K1, Canada

ARTICLE INFO

Article history:
Available online xxxx

Keywords:
Cognitive tracking radar
Dynamic programming
Integration approximation
Cubature Kalman filter
Fore-active tracking radar

ABSTRACT

In Haykin (2006) [8], the idea of Cognitive Radar was described for the first time. Four essential points were emphasized in that seminal paper: Bayesian filtering in the receiver, dynamic programming in the transmitter, memory, and global feedback to facilitate computational intelligence. This paper provides a first step towards designing a cognitive radar for tracking applications by presenting a fore-active tracking radar; a radar that utilizes its previous measurements and actions to optimize its transmitted waveform (Haykin, 2011 [11]). In our design, the emphasis is being placed on the cubature Kalman filter to approximate the Bayesian filter in the receiver, approximate dynamic programming for transmit-waveform selection in the transmitter, and global feedback embodying the transmitter, the radar environment, and the receiver all under one overall feedback loop. Simulation results, based on the tracking of an object falling in space, are presented, which substantiate practical validity of the superior performance of a fore-active tracking radar over a traditional active radar with fixed waveform.

1. Introduction

In Haykin [8], the idea of Cognitive Radar was described for the first time in a seminal paper. Motivation for this new idea was the echo-location system of a bat. Another equally compelling motivation for cognition is the visual brain. In most basic terms, the visual brain is characterized by two important features, perception of the environment (the world) in one part of the brain and action to control the environment in a separate part of the brain [6]. The net result of these two functions, working together in a coordinated fashion, is the perception-action cycle; this basic cycle is indeed the brain's counterpart to the information-processing cycle in a cognitive radar that was described in Haykin [8]. Another compelling way to see the close relationship between cognitive radar and the visual brain is to examine the coding–decoding function. Here again, it is rather striking to find that this basic property of cognition in the brain and its counterpart in cognitive radar are ever so closely analogous [9]. The point that we are trying to emphasize here is that if we are to build up our knowledge about the fundamentals of cognitive radar, there is much that we can learn from the mammalian brain.

With optimal performance as the goal, the ideal way to build a cognitive radar is to look to the optimal Bayesian filter [12] as the central functional block in the receiver for perception of the environment, and Bellman's dynamic programming [3] as the central functional block in the transmitter for action to control the environment. Naturally, there has to be feedback from the receiver to the transmitter to make it possible for the receiver to send information about the environment to the transmitter. In so doing, global feedback, embodying the two parts of the radar system and the environment under a single overall loop operating in an *on-line* manner, and with it the radar becomes computationally intelligent to some extent. Here again, if we are to examine the visual brain, we will find that, unlike perception and action, there is no single functional block that takes care of intelligence; rather, this important function is distributed through feedback across many parts of the brain.

In the light of cognition as an influential factor in the design of next generation of radar, we now have three classes of radars [11]:

- *Traditional active* radar that has no feedback from the receiver to the receiver and therefore the transmit-waveform is fixed.
- *Fore-active* radar that utilizes the information fed back from the transmitter to choose its transmit waveform.
- The *cognitive* radar that expands on fore-active radar by having memory, attention and enhanced intelligence.

The radar system presented in this manuscript is an example of a fore-active radar that paves the way towards achieving the first step towards cognition.

With this introduction on the analogy between the visual brain and cognitive radar, we may now briefly describe how the rest of the paper is organized: Section 2 of the paper describes a baseband model of the signal transmission link that extends from the continuous-time transmitter output to the discrete-time input of

* Corresponding author.
E-mail addresses: haykin@mcmaster.ca (S. Haykin), ziama@mcmaster.ca (A. Zia), yxue@grads.ece.mcmaster.ca (Y. Xue), aienkaran@grads.ece.mcmaster.ca (I. Arasaratnam).

1051-2004/$ – see front matter
doi:10.1016/j.dsp.2011.01.004

the cubature Kalman filter (CKF) in the receiver; we refer to this extension as the forward transmission path. Brief description of the CKF approximation to the optimal Bayesian filter is presented in Section 3; it is the CKF that perceives the environment, thereby extracting the information about state of the radar target to send feedback information about it to the transmitter. Section 4 outlines the basic fore-active tracking radar (FATR) problem with finite depth of horizon, thereby setting the stage for the formulation of a dynamic-programming (DP) algorithm for action to control the receiver via the environment through a waveform-selection process. This linkage from the receiver output to the transmitter output is referred as the feedback transmission path. Section 4 also discusses two other issues: cubature rule based approximation for the cost-to-go function needed for the DP algorithm, followed by computational issues involved in implementing it. Section 5 describes a computer experiment to evaluate the FATR performance under a classic tracking scenario that focuses on a target falling in space; the root mean-square error (RMSE) for the state is displayed in the simulation results for different state parameters. The concluding section summarizes the important findings in the paper. Notations used in the paper are summarized in Appendix A at the end of this paper; and Appendix B addresses an important approximation in evaluating the cost function.

2. Analog-to-digital baseband model of radar signal transmission

A commonly used method to control selection of the transmit-waveform is to equip the transmitter with a digitally implementable waveform generator that embodies a prescribed library of waveforms. To elaborate, when we speak of a baseband model, we mean a band of frequencies determined by the waveform-generator's spectral content. For designing the waveform generator, we have opted for linear frequency modulation (LFM) combined with Gaussian pulse for amplitude modulation. With f_c denoting the carrier frequency of the transmitted radar signal, $s_T(t)$, we may now use complex baseband theory to express it as follows:

$$s_T(t) = \sqrt{2}\,\mathrm{Re}\left\{\sqrt{E_T}\tilde{s}(t)\exp(j2\pi f_c t)\right\}, \tag{1}$$

where E_T is the transmitted signal energy, and $\tilde{s}(t)$ is the complex envelope of $s_T(t)$ [7]:

$$\tilde{s}(t) = \left(\pi\lambda^2\right)^{-\frac{1}{4}}\exp\left(-\left(\frac{1}{2\lambda^2} - jb\right)t^2\right) \tag{2}$$

with $|t| \leqslant T/2 + t_f$ where $t_f \ll T/2$ is the rise and fall time, λ is the duration of the Gaussian envelope, and b is a scalar denoting the chirp rate. We use the vector $\boldsymbol{\theta} = [\lambda, b]$ to denote the two transmit waveform parameters that will be optimized by the waveform-selection algorithm. We discretize the possible range of transmit waveform parameters into a two-dimensional grid. Each point in this grid corresponds to a transmit waveform. All waveforms correspond to all the grid points from our transmit waveform library.

The radar echo reflected from the target received at the receiver input is correspondingly defined by

$$r(t) = s_R(t) + n(t), \tag{3}$$

where $s_R(t)$ is the signal component of $r(t)$ and $n(t)$ is the additive white Gaussian noise, both of which are centered on the carrier frequency f_c. Invoking complex baseband theory, we may define $s_R(t)$ as follows:

$$s_R(t) = \sqrt{2}\,\mathrm{Re}\left[\sqrt{E_R}\tilde{s}(t-\tau)\exp\left(j2\pi\left(f_c t + \nu t\right)\right)\right], \tag{4}$$

where E_R is the received signal energy; $\tau = 2\rho/c$ is the delay of the received signal where ρ is the range of the target, and c denotes the speed of electromagnetic wave propagation (i.e. the speed of light); ν is the Doppler shift defined by $-2f_c\dot{\rho}/c$ with $\dot{\rho}$ denoting the range rate of the target, assuming that the target is moving toward the radar. Finally, $\tilde{n}(t)$ denotes the complex envelope of the noise $n(t)$ at the receiver input. Throughout the paper, it is assumed that the transmitted radar signal is narrowband, which means the complex envelopes $\tilde{s}(t)$ and $\tilde{n}(t)$ in the baseband model occupy a frequency band small in comparison to the carrier frequency f_c.

The idea behind baseband modeling, exemplified by the complex envelopes $\tilde{s}(t)$ and $\tilde{n}(t)$, is that both of these components are low-pass in their spectral characteristics, whereas the band-pass transmitted signal $s_T(t)$ and received signal $r(t)$ are more difficult to handle. Most importantly, baseband modeling dispenses with the carrier frequency f_c and there is no loss of information in basing the radar signal analysis on complex envelopes.

2.1. Bank of matched filters and envelope detectors

At the front end of the receiver, typically, we have a bank of matched filters. The impulse response of a matched filter is defined by the conjugate of the complex transmitted signal envelope $\tilde{s}(t)$, shifted in time as well as frequency by scaled versions of desired time- and frequency-resolutions, respectively. Recognizing that a matched filter is basically equivalent to a correlator, it follows that the bank of matched filters acts as a time-frequency correlator of the complex transmitted signal envelope with itself. In the absence of receiver noise, the squared magnitude of this correlation constitutes the ambiguity function [16]. Every matched filter in the filter bank is therefore followed by a square-law envelope detector. The resulting real-valued two-dimensional output of each envelope detector, involving time delay and Doppler shift, defines an interpulse vector denoted by $\mathbf{z}_k$, where the subscript k denotes discrete time. This vector performs the role of *measurement vector* in the state-space model of the radar target, discussed next.

2.2. State-space model of the target

There are two equations in the state-space model of a radar target:

- **System equation**, which describes evolution of the target's state across time in accordance with the nonlinear equation:

$$\mathbf{x}_k = \mathbf{f}(\mathbf{x}_{k-1}) + \mathbf{v}_k, \tag{5}$$

  where $\mathbf{x}_k$ denotes the *state* of the radar target at discrete time k, and $\mathbf{v}_k$ denotes the additive system noise accounting for environmental uncertainty about the target. The state of the target can be chosen in a manner depending on the problem. For instance it can include the position, the velocity and the acceleration of the target. The state space for our case study problem, i.e. tracking of a falling object, is the object altitude, velocity and the ballistic coefficient.
- **Measurement equation**, which describes dependence of the measurement vector $\mathbf{z}_k$ on the state $\mathbf{x}_k$ as shown by

$$\mathbf{z}_k = \mathbf{h}(\mathbf{x}_k) + \mathbf{w}_k(\boldsymbol{\theta}_{k-1}), \tag{6}$$

  where the vector $\mathbf{w}_k(\boldsymbol{\theta}_{k-1})$ denotes the measurement noise that acts as the *driving force*. It is in the dependence of this noise on the waveform-parameter vector $\boldsymbol{\theta}_{k-1}$ that the transmitter influences accuracy of the state estimation in the receiver. The transmit waveform parameters at time k.

Application of the state-space model described in (5) and (6) hinges on the following four basic assumptions:

Please cite this article in press as: S. Haykin et al., Control theoretic approach to tracking radar: First step towards cognition, Digital Signal Process. (2011), doi:10.1016/j.dsp.2011.01.004

- First, the nonlinear vectorial functions $\mathbf{f}(\cdot)$ and $\mathbf{h}(\cdot)$ in (5) and (6) are both smooth and otherwise arbitrary.
- Second, the system noise $\mathbf{v}_k$ and measurement noise $\mathbf{w}_k$ are zero-mean Gaussian distributed and statistically independent of each other. The Gaussian assumption is valid for cases where the thermal noise is the only source of measurement noise. Otherwise, it is a convenient assumption for mathematical tractability in derivation of state-space estimation equations.
- Third, the covariance matrix of system noise is known.
- Fourth, the state is independent from both the system noise and measurement noise.

Examining (5) and (6), we immediately see that the state $\mathbf{x}_k$ is *hidden* from the observer, and the challenge for the receiver is to exploit dependence of the measurement vector on the state to compute an estimate of the state and do so in a sequential on-line manner.

With this objective in mind, we need to determine statistical characteristics of the measurement noise $\mathbf{w}_k$. To this end, we first recognize that the measurement noise covariance is dependent on the parameter $\boldsymbol{\theta}_{k-1}$ of the waveform generator in the transmitter [13], hence the notation $\mathbf{R}(\boldsymbol{\theta}_{k-1})$ for this covariance. Moreover, the inverse of the *Fisher information matrix* is the *Cramér–Rao lower bound* on the state estimation error covariance matrix for unbiased estimator [15]. Denoting the Fisher information matrix by $\mathbf{J}$, we may consider the inverse matrix $\mathbf{J}^{-1}$ as a suitable characterization for optimal waveform selection, and thus write

$$\mathbf{R}(\boldsymbol{\theta}_{k-1}) = \boldsymbol{\Gamma}\mathbf{J}^{-1}(\boldsymbol{\theta}_{k-1})\boldsymbol{\Gamma}, \tag{7}$$

where $\boldsymbol{\Gamma}$ is a symmetric matrix defined by

$$\boldsymbol{\Gamma} \triangleq \operatorname{diag}\left[\frac{c}{2}, \frac{c}{2f_c}\right]. \tag{8}$$

For convenience of presentation, it is desirable to separate the contribution of the waveform parameter vector in the Fisher information matrix from the received signal energy-to-noise spectral density ratio (i.e. the SNR) defined by

$$\eta = \frac{2E_R}{N_0}, \tag{9}$$

where N_0 is the spectral density of the complex noise envelope $\tilde{n}(t)$. To this end, we write

$$\mathbf{J}(\boldsymbol{\theta}_{k-1}) = \eta\mathbf{U}(\boldsymbol{\theta}_{k-1}). \tag{10}$$

Accordingly, we may rewrite (7) in the desired form [14]

$$\mathbf{R}(\boldsymbol{\theta}_{k-1}) = \frac{1}{\eta}\boldsymbol{\Gamma}\mathbf{U}^{-1}(\boldsymbol{\theta}_{k-1})\boldsymbol{\Gamma}, \tag{11}$$

with the matrix $\mathbf{U}(\boldsymbol{\theta})$ being merely a scaled version of the Fisher information matrix $\mathbf{J}(\boldsymbol{\theta})$, this new matrix is a symmetric matrix whose three elements are described as mean-square values of the following errors:

- the Doppler estimation error,
- the cross Doppler-delay estimation error, and
- the delay estimation error.

In Kershaw and Evans [13], it is shown that for the transmit waveform, combining linear frequency modulation with Gaussian amplitude modulation, the measurement noise covariance matrix is defined by

$$\mathbf{R}(\boldsymbol{\theta}_{k-1}) = \begin{bmatrix} \frac{c^2\lambda^2}{2\eta} & -\frac{c^2 b\lambda^2}{2\pi f_c\eta} \\ -\frac{c^2 b\lambda^2}{2\pi f_c\eta} & \frac{c^2}{(2\pi f_c)^2\eta}\left(\frac{1}{2\lambda^2} + 2b^2\lambda^2\right) \end{bmatrix}. \tag{12}$$

It is important to note however that this formula for $\mathbf{R}(\boldsymbol{\theta}_{k-1})$ is valid so long as the assumption that the energy per transmitted waveform remains constant from one cycle to the next. Otherwise, we would have to expand the waveform parameter vector $\boldsymbol{\theta}_{k-1}$ by adding a new variable η_{k-1}.

3. Cubature Kalman filter for target state estimation

As stated previously in Section 1, the optimal Bayesian filter is the ideal tool for tracking the target's state in the radar receiver. Unfortunately, when the state-space model is nonlinear as it is in (5) and (6), the Bayesian filter is no longer computationally feasible, hence the practical need for its approximation. To this end, the cubature Kalman filter is the closest known approximation to the Bayesian filter that could be designed in a nonlinear setting under the key assumption: The predictive density of the joint state-measurement random variable is Gaussian [1]. Under this assumption, the Bayesian filter reduces to the problem of how to compute moment integrals whose integrands are of the following form:

$$\text{nonlinear function} \times \text{Gaussian}. \tag{13}$$

To numerically compute integrals whose integrands are of this form, we use a rule described next.

3.1. The cubature rule of third degree

Consider an example of the integrand described in (13), which consists of the nonlinear function $\mathbf{f}(\mathbf{x})$ multiplied by a multivariate Gaussian density denoted by $\mathcal{N}(\mathbf{x}; \boldsymbol{\mu}, \boldsymbol{\Sigma})$, where $\boldsymbol{\mu}$ is the mean and $\boldsymbol{\Sigma}$ is the covariance. According to the third-degree cubature rule [5], the resulting integral may be approximated as follows:

$$\int_{\mathbb{R}^n} \mathbf{f}(\mathbf{x})\mathcal{N}(\mathbf{x}; \boldsymbol{\mu}, \boldsymbol{\Sigma})\, d\mathbf{x} \approx \frac{1}{2n}\sum_{i=1}^{2n} \mathbf{f}(\boldsymbol{\mu} + \sqrt{\boldsymbol{\Sigma}}\boldsymbol{\alpha}_i), \tag{14}$$

where a square-root factor of the state-estimation error covariance $\boldsymbol{\Sigma}$ satisfies the factorization $\boldsymbol{\Sigma} = \sqrt{\boldsymbol{\Sigma}}\sqrt{\boldsymbol{\Sigma}}^T$; the set of $2n$ cubature points is given by

$$\boldsymbol{\alpha}_i = \begin{cases} \sqrt{n}\,\mathbf{e}_i, & i = 1, 2, \ldots, n, \\ -\sqrt{n}\mathbf{e}_{i-n}, & i = n+1, n+2, \ldots, 2n, \end{cases} \tag{15}$$

with $\mathbf{e}_i \in \mathbb{R}^n$ denoting the i-th elementary column vector. The CKF specifically uses the third-degree cubature rule to numerically compute Gaussian weighted integrals. This rule is exact for integrands being polynomials of degree up to three or any odd integer.

Here we present the CKF's two-step update cycle, namely, the time update and the measurement update as described next.

3.2. Time update

In the time-update step, the CKF [1] computes the mean $\hat{\mathbf{x}}_{k|k-1}$ and the associated covariance $\mathbf{P}_{k|k-1}$ of the Gaussian predictive density numerically using cubature rules. We write the predicted mean

$$\hat{\mathbf{x}}_{k|k-1} = \mathbb{E}[\mathbf{x}_k|D_{k-1}], \tag{16}$$

where $\mathbb{E}[\cdot]$ is the statistical expectation operator and D_k is the history of input-measurement pairs available up to time k. Substituting the system equation (5) into (16) yields

$$\hat{\mathbf{x}}_{k|k-1} = \mathbb{E}\big[\mathbf{f}(\mathbf{x}_{k-1}) + \boldsymbol{\nu}_k|D_{k-1}\big]. \tag{17}$$

Because $\boldsymbol{\nu}_k$ is assumed to be zero-mean and uncorrelated with the measurement sequence, we get

Please cite this article in press as: S. Haykin et al., Control theoretic approach to tracking radar: First step towards cognition, Digital Signal Process. (2011), doi:10.1016/j.dsp.2011.01.004

$$\hat{\mathbf{x}}_{k|k-1} = \mathbb{E}\big[\mathbf{f}(\mathbf{x}_{k-1})|D_{k-1}\big] = \int_{\mathbb{R}^{N_x}} \mathbf{f}(\mathbf{x}_{k-1})\, p(\mathbf{x}_{k-1}|D_{k-1})\, d\mathbf{x}_{k-1} = \int_{\mathbb{R}^{N_x}} \mathbf{f}(\mathbf{x}_{k-1})\mathcal{N}(\mathbf{x}_{k-1}; \hat{\mathbf{x}}_{k-1|k-1}, \mathbf{P}_{k-1|k-1})\, d\mathbf{x}_{k-1}, \tag{18}$$

where, as before, $\mathcal{N}(.;.,.)$ is the conventional symbol for a Gaussian density. Similarly, we obtain the associated error covariance

$$\mathbf{P}_{k|k-1} = \mathbb{E}\big[(\mathbf{x}_k - \hat{\mathbf{x}}_{k|k-1})(\mathbf{x}_k - \hat{\mathbf{x}}_{k|k-1})^T|D_{k-1}\big] = \int_{\mathbb{R}^{N_x}} \mathbf{f}(\mathbf{x}_{k-1})\mathbf{f}^T(\mathbf{x}_{k-1})\mathcal{N}(\mathbf{x}_{k-1}; \hat{\mathbf{x}}_{k-1|k-1}, \mathbf{P}_{k-1|k-1})\, d\mathbf{x}_{k-1} - \hat{\mathbf{x}}_{k|k-1}\hat{\mathbf{x}}_{k|k-1}^T + \mathbf{Q}_{k-1}, \tag{19}$$

where $\mathbf{Q}_k$ is the covariance of system noise $\mathbf{v}_k$.

3.3. Measurement update

Recognizing that the so-called innovation process is not only white but also zero-mean Gaussian when the additive measurement noise is Gaussian, the predicted measurement may be estimated in the least-squares error sense. In this case, we write the predicted measurement density also called the filter likelihood density, as follows

$$p(\mathbf{z}_k|D_{k-1}) = \mathcal{N}(\mathbf{z}_k; \hat{\mathbf{z}}_{k|k-1}, \mathbf{P}_{\mathbf{zz},k|k-1}), \tag{20}$$

where the predicted measurement itself and the associated covariance are respectively given by

$$\hat{\mathbf{z}}_{k|k-1} = \int_{\mathbb{R}^{N_x}} \mathbf{h}(\mathbf{x}_k)\mathcal{N}(\mathbf{x}_k; \hat{\mathbf{x}}_{k|k-1}, \mathbf{P}_{k|k-1})\, d\mathbf{x}_k, \tag{21}$$

$$\mathbf{P}_{\mathbf{zz},k|k-1} = \int_{\mathbb{R}^{N_x}} \mathbf{h}(\mathbf{x}_k)\mathbf{h}^T(\mathbf{x}_k)\mathcal{N}(\mathbf{x}_k; \hat{\mathbf{x}}_{k|k-1}, \mathbf{P}_{k|k-1})\, d\mathbf{x}_k - \hat{\mathbf{z}}_{k|k-1}\hat{\mathbf{z}}_{k|k-1}^T + \mathbf{R}(\boldsymbol{\theta}_{k-1}). \tag{22}$$

Accordingly, we may write the Gaussian conditional density of the joint state and the measurement:

$$p\big([\mathbf{x}_k^T \quad \mathbf{z}_k^T]^T|D_{k-1}\big) = \mathcal{N}\left(\begin{pmatrix}\hat{\mathbf{x}}_{k|k-1}\\ \hat{\mathbf{z}}_{k|k-1}\end{pmatrix}, \begin{pmatrix}\mathbf{P}_{k|k-1} & \mathbf{P}_{\mathbf{xz},k|k-1}\\ \mathbf{P}_{\mathbf{xz},k|k-1}^T & \mathbf{P}_{\mathbf{zz},k|k-1}\end{pmatrix}\right), \tag{23}$$

where the cross-covariance

$$\mathbf{P}_{\mathbf{xz},k|k-1} = \int_{\mathbb{R}^{N_x}} \mathbf{x}_k\mathbf{h}^T(\mathbf{x}_k)\mathcal{N}(\mathbf{x}_k; \hat{\mathbf{x}}_{k|k-1}, \mathbf{P}_{k|k-1})\, d\mathbf{x}_k - \hat{\mathbf{x}}_{k|k-1}\hat{\mathbf{z}}_{k|k-1}^T. \tag{24}$$

On the receipt of a new measurement $\mathbf{z}_k$, the CKF computes the posterior density $p(\mathbf{x}_k|D_k)$ from (23) yielding

$$p(\mathbf{x}_k|D_k) = \frac{p(\mathbf{x}_k, \mathbf{z}_k|D_{k-1})}{p(\mathbf{z}_k|D_{k-1})} = \mathcal{N}(\mathbf{x}_k; \hat{\mathbf{x}}_{k|k}, \mathbf{P}_{k|k}), \tag{25}$$

where

$$\hat{\mathbf{x}}_{k|k} = \hat{\mathbf{x}}_{k|k-1} + \mathbf{G}_k(\mathbf{z}_k - \hat{\mathbf{z}}_{k|k-1}), \tag{26}$$

$$\mathbf{P}_{k|k} = \mathbf{P}_{k|k-1} - \mathbf{G}_k\mathbf{P}_{\mathbf{zz},k|k-1}\mathbf{G}_k^T, \tag{27}$$

with the *Kalman gain* being defined by

$$\mathbf{G}_k = \mathbf{P}_{\mathbf{xz},k|k-1}\mathbf{P}_{\mathbf{zz},k|k-1}^{-1}. \tag{28}$$

In sum, the CKF numerically computes Gaussian weighted integrals that are present in (18)–(19), (21)–(22) and (24) using cubature rules.

4. Dynamic programming for waveform selection

Previously we remarked that the measurement covariance in state equation (6) depends on the transmitted waveform parameter vector $\boldsymbol{\theta} = [\lambda, b]$, which applies to LFM with Gaussian amplitude modulation. Hence, if the waveform parameters are selected optimally, any *action* taken by the transmitter will be regarded as an optimal *reaction* to the environment perceived by the receiver. With this point in mind, we may now address the algorithmic formulation for waveform selection in the transmitter. In effect, the new algorithm assumes the role of a controller in a nonlinear feedback system that tunes the transmit-waveform parameters so as to tame the behavior of the receiver in an effort to minimize the tracking errors in some statistical sense.

The perception-action cycle. This cycle, representing the first step towards cognition, operates as follows:

- The transmitter illuminates the environment at time k by generating a waveform whose parameters are defined by $\boldsymbol{\theta}_k$.
- Assuming a unit-time delay to account for propagation from the transmitter to the receiver, the measurement at the receiver front is denoted by $\mathbf{z}_{k+1}$.
- The CKF in the receiver operates on $\mathbf{z}_{k+1}$ to produce a one-step predicted estimate of the true state, denoted by $\hat{\mathbf{x}}_{k+1|k}$. The feedback sent to the transmitter is correspondingly based on the predicted state estimate error vector, denoted by the covariance matrix $\mathbf{P}_{k+1|k}$ which is computable given the measurement $\mathbf{z}_k$.
- With this covariance matrix at hand, the transmitter receives the covariance matrix by one time step to compute the filtered state-error covariance matrix $\mathbf{P}_{k+1|k+1}$. As noted previously by Kershaw and Evans [13], there is only one unknown in the computation of $\mathbf{P}_{k+1|k+1}$ and that is the update waveform-parameter vector $\boldsymbol{\theta}_{k+1}$ which, of course, is not available at time k.
- To solve for $\boldsymbol{\theta}_k$ we look to dynamic programming to find the particular set of parameters for which the mean squared state estimate error vector, that is the trace of $\mathbf{P}_{k+1|k+1}$, is minimized.
- Now, with $\boldsymbol{\theta}_k$ at hand, the stage is set for the next perception-action cycle to be performed at time $k+1$ and so in goes on.

Before proceeding further, two important remarks deserve particular attention:

- First, when a cognitive tracking radar is viewed as a feedback control system, the basic perception-action cycle is replaced by a measurement-waveform selection cycle, that is $(\mathbf{z}_k, \boldsymbol{\theta}_k)$, where k denotes the current cycle. In other words, the measurement $\mathbf{z}_k$ made by the receiver at cycle k leads to waveform selection $\boldsymbol{\theta}_k$ in the transmitter at the next cycle $k+1$.
- Second, the state of the target is *hidden* from the receiver, which, in turn, poses a practical problem in the following sense: The formulation of Bellman's dynamic programming not only demands that the environment be Markovian but also the controller has perfect knowledge of the state. In reality, however, the transmitter of a radar tracker has an *imperfect* estimate of the state reported to it by the receiver. Accordingly, we are faced with an *imperfect state-information problem*.

Please cite this article in press as: S. Haykin et al., Control theoretic approach to tracking radar: First step towards cognition, Digital Signal Process. (2011), doi:10.1016/j.dsp.2011.01.004

To resolve this problem, we follow [4] by introducing a new information state vector defined by

$$\mathbf{I}_k \triangleq (\mathbf{Z}_k, \boldsymbol{\Theta}_{k-1}), \quad \text{with } \mathbf{I}_0 = \mathbf{z}_0, \tag{29}$$

where

$$\mathbf{Z}_k = [\mathbf{z}_1, \mathbf{z}_2, \ldots, \mathbf{z}_k], \tag{30}$$

$$\boldsymbol{\Theta}_{k-1} = [\boldsymbol{\theta}_0, \boldsymbol{\theta}_1, \ldots, \boldsymbol{\theta}_{k-1}]. \tag{31}$$

From these three equations, we readily obtain the recursion

$$\mathbf{I}_{k+1} = (\mathbf{I}_k, \mathbf{z}_{k+1}, \boldsymbol{\theta}_k), \tag{32}$$

which may be viewed as the state evolution of a new dynamic system with perfect-state information, and therefore applicable to dynamic programming. According to (32), we may say:

- $\mathbf{I}_k$ is the current value of the state;
- $\boldsymbol{\theta}_k$ is the next waveform parameter vector computed at time k and to be chosen for transmission at time k which will be received by the transmitter at time $k+1$;
- the measurement $\mathbf{z}_{k+1}$ is viewed as a random disturbance resulting from the control decision $\boldsymbol{\theta}_k$; and
- note that the terminology adopted in (32) is consistent with the system equation (5).

The information-processing cycle. At any cycle time k, the waveform-selection algorithm seeks to find the set of best waveform parameters by minimizing a cost-to-go function for a rolling horizon of L steps, that is, to minimize the cost incurring in steps k: $k+L-1$. Denoting the control policy for the next L steps by $\pi_k = \{\mu_k, \ldots, \mu_{k+L-1}\}$ with the policy function $\mu(\mathbf{I}_k) = \boldsymbol{\theta}_k \in \mathcal{P}_k$ mapping the information vector into an action in the waveform library $\mathcal{P}_k$, we wish to find a policy π_k at time k corresponding to the solution of the following minimization:

$$\min_{\pi_k} \mathbb{E}\left[\sum_{i=k}^{k+L-1} g\big(\mathbf{I}_i, \mu_i(\mathbf{I}_k)\big)\right], \tag{33}$$

where the cost function $g(\cdot)$ inside the summation is defined as the tracking *expected* mean-square error (MSE):

$$g(\mathbf{I}_k, \mu_k) = \mathbb{E}_{\mathbf{x}_{k+1}, \mathbf{z}_{k+1}|\mathbf{I}_k, \boldsymbol{\theta}_k}\big[(\mathbf{x}_{k+1} - \hat{\mathbf{x}}_{k+1|k+1})^T (\mathbf{x}_{k+1} - \hat{\mathbf{x}}_{k+1|k+1})\big], \tag{34}$$

where $\hat{\mathbf{x}}_{k+1|k+1}(\mathbf{I}_k, \mathbf{x}_{k+1}, \mathbf{z}_k, \boldsymbol{\theta}_k)$ is the posterior *expected* state estimation given the selected parameter vector $\boldsymbol{\theta}_k$. Obviously, for an L-step dynamic-programming algorithm, we need to predict L-steps ahead, which also means that accurate performance of the predictor in the receiver is of crucial to performance of the cognitive tracking radar.

To elaborate more about the behavior of the cognitive tracking radar system, we may refer to Fig. 1, where the information flow is classified into two paths:

(1) **Feedforward transmission path for optimal estimation of the estimated state in the receiver**. In this path, the transmitter has already selected the waveform parameter vector $\boldsymbol{\theta}_k$. The receiver then builds on previous knowledge of $\boldsymbol{\theta}_k$ and current observable $\mathbf{z}_k$ available at time k to locally optimize the state estimation.

(2) **Feedback transmission path for updating the waveform selection in the transmitter**. Given the mean-square error computed at the receiver (CKF) output at time k, the requirement is to find the policy μ_k that selects $\boldsymbol{\theta}_k$ for the next signal transmission at time $k+1$.

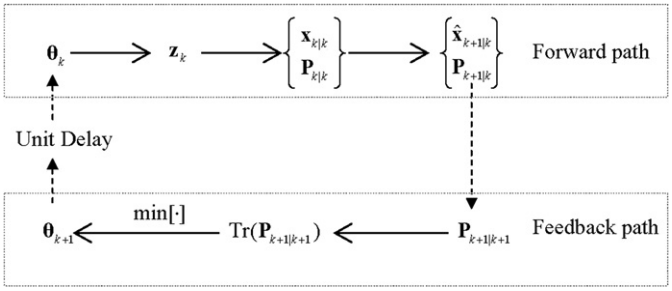

Fig. 1. Information flow in fore-active tracking radar.

Note that in Fig. 1 we plot the signal flow by looking one-step into the future. The computation starts with the initial condition $(\mathbf{z}_0, \boldsymbol{\theta}_0)$ and proceeds by computing $\boldsymbol{\theta}_1$, and so on. When there is provision of a horizon looking more steps into the future, we will have a general optimization problem. This optimization is solved by a recursive dynamic-programming (DP) algorithm at time k, which is made up two parts (see [4] for details):

Terminal point:

$$\mathcal{J}(\mathbf{I}_{L-1}, \mu_{L-1}) = \inf_{\boldsymbol{\theta}_{L-1} \in \mathcal{P}_{L-1}} g(\mathbf{I}_{L-1}, \mu_{L-1}). \tag{35}$$

Intermediate points:

$$\mathcal{J}(\mathbf{I}_k, \mu_k) = \inf_{\boldsymbol{\theta}_k \in \mathcal{P}_k} \big(g(\mathbf{I}_k, \mu_k) + \mathbb{E}_{\mathbf{z}_{k+1}|\mathbf{I}_k, \boldsymbol{\theta}_k}[\mathcal{J}_{k+1}]\big) \tag{36}$$

for $p = k, \ldots, k+L-1$, where $\mathcal{J}_p = \mathcal{J}(\mathbf{I}_p, \mu_p)$. With (35) pertaining to the terminal point, (36) pertains to the intermediate points that go backward from the terminal point in $(L-1)$ steps. The optimal policy $\{\mu_k^*, \ldots, \mu_{k+L-1}^*\}$ is obtained in the following two-step manner:

- We first minimize the terminal point (35) for every possible value of the information vector $\mathbf{I}_{k+L-1}$ to obtain μ_{k+L-1}^*. Meanwhile, $\mathcal{J}_{k+L-1}$ is also computed;
- Then, $\mathcal{J}_{k+L-1}$ is substituted into the calculation of the intermediate points (36) to obtain μ_{k+L-1}^* over every possible value of $\mathcal{J}_{k+L-2}$. This step is repeated until we reach to the initial point with μ_k.

In what follows, we apply two approximations to simplify the DP algorithm.

4.1. Approximation of the cost function $g(\cdot)$

Inclusion of the state $\mathbf{x}_{k+1}$ under the expectation defined in (34) speaks for itself. As for the observable $\mathbf{z}_{k+1}$, its inclusion under the expectation is justified on the following ground: As shown in the second line of (34), the estimate $\hat{\mathbf{x}}_{k+1|k+1}$ depends on $\mathbf{z}_{k+1}$, which itself depends nonlinearly on $\mathbf{x}_{k+1}$. Consequently, it is difficult to evaluate this expectation. The best we may therefore do is to approximate the cost $g(\mathbf{I}_k, \mathbf{z}_k)$ as shown by

$$g(\mathbf{I}_k, \mu_k) \approx \mathrm{Tr}(\mathbf{P}_{k+1|k+1}), \tag{37}$$

where $\mathrm{Tr}(\cdot)$ is an operator that extracts the trace of the enclosed covariance $\mathbf{P}_{k+1|k+1}$; see Appendix B for detailed derivation of this approximate formula.

4.2. Measurement-space approximation

The measurement space (i.e., the control space for the waveform selection algorithm) is an infinite-dimensional continuous-valued space. Moreover, the dimension of this space grows exponentially with depth of the optimization horizon L. In fact, at each

Please cite this article in press as: S. Haykin et al., Control theoretic approach to tracking radar: First step towards cognition, Digital Signal Process. (2011), doi:10.1016/j.dsp.2011.01.004

step of the optimization, we need to examine an infinite number of possibilities that the perfect state information vector $\mathbf{I}_{k+1}$ can evolve to the next step in time. To simplify this computation, we use the same approximation technique used in development of the CKF in Section 3 by approximating the expectation operation in (34) using the third-degree cubature rule. According to the CKF formulation, the predicted measurement $\mathbf{z}_{k+1}$ is Gaussian-distributed with mean $\hat{\mathbf{z}}_{k+1|k}$ as in (21) and covariance $\mathbf{P}_{\mathbf{zz},k+1|k}$ in (22). Therefore the expectation term in (34) may now be written as

$$\begin{aligned}&\mathbb{E}_{\mathbf{z}_{k+1}|\mathbf{I}_k,\boldsymbol{\theta}_k}\big[\mathrm{Tr}(\mathbf{P}_{k+1|k+1})\big]\\&=\int_{\mathbf{z}_{k+1}} p(\mathbf{z}_{k+1}|\mathbf{I}_k,\boldsymbol{\theta}_k)\,\mathrm{Tr}(\mathbf{P}_{k+1|k+1})\,d\mathbf{z}_{k+1}\\&=\int_{\mathbf{z}_{k+1}} \mathcal{N}(\hat{\mathbf{z}}_{k+1|k},\mathbf{P}_{\mathbf{zz},k+1|k})\,\mathrm{Tr}(\mathbf{P}_{k+1|k+1})\,d\mathbf{z}_{k+1}.\end{aligned}\tag{38}$$

Approximating the integral in (38) using the cubature rule of (14), we obtain

$$\begin{aligned}&\mathbb{E}_{\mathbf{z}_{k+1}|\mathbf{I}_k,\boldsymbol{\theta}_k}\big[\mathrm{Tr}(\mathbf{P}_{k+1|k+1})\big]\\&\approx\mathrm{Tr}\left(\frac{1}{2N_z}\sum_{i=1}^{2N_z}\mathbf{P}_{k+1|k+1}\big(\hat{\mathbf{z}}_{k+1|k}+\mathbf{P}^{1/2}_{\mathbf{zz},k+1|k}\boldsymbol{\alpha}_i\big)\right),\end{aligned}\tag{39}$$

where $\mathbf{P}_{k+1|k+1}$ is expressed as a function of $(\hat{\mathbf{z}}_{k+1|k}+\mathbf{P}^{1/2}_{\mathbf{zz},k+1|k}\boldsymbol{\alpha}_i)$ and $\mathbf{P}^{1/2}_{\mathbf{zz},k+1|k}$ is the square root of the covariance matrix $\mathbf{P}_{\mathbf{zz},k+1|k}$ and the cubature points $\boldsymbol{\alpha}_i$ are defined in accordance with (15).

Thus, using the approximation of (39), the DP algorithm is simplified into the following pair of equations:

Terminal point:

$$\mathcal{J}(\mathbf{I}_{k+L-1},\mu_{k+L-1})=\inf_{\boldsymbol{\theta}_{k+L-1}\in\mathcal{P}_{k+L-1}}\mathrm{Tr}(\mathbf{P}_{k+L-1|k+L-1}).\tag{40}$$

Intermediate points:

$$\begin{aligned}&\mathcal{J}(\mathbf{I}_k,\mu_k)\\&=\inf_{\boldsymbol{\theta}_k\in\mathcal{P}_k}\mathrm{Tr}\left(\mathbf{P}_{k|k}+\frac{1}{2N_z}\sum_{i=1}^{2N_z}\mathbf{P}_{k+1|k+1}\big(\hat{\mathbf{z}}_{k+1|k}+\mathbf{P}^{1/2}_{\mathbf{zz},k+1|k}\boldsymbol{\alpha}_i\big)\right)\end{aligned}\tag{41}$$

for $k=1,\ldots,L-1$, where (40) denotes the terminal point and (41) denotes the intermediate points going backward. The intermediate points (41) collapse to the terminal point (40) if and only if $L=1$. In other words, the terminal point (40) computes the cost-to-go function looking $L-1$ cycles into the future, where L is the prescribed horizon. Then, starting with the computed cost $\mathcal{J}(\mathbf{I}_k,\mu_k)$, the DP algorithm (41) computes the sequence of cost-to-go functions by going backward step-by-step till we arrive at the present cycle time k.

4.3. Special case: dynamic optimization

The DP algorithm of (40) and (41) includes dynamic optimization of the FATR as a special case. For the case when there is no provision of a horizon looking into the future of $L\geqslant 2$, the terminal point in (41) defines the dynamic optimization algorithm. Then, there is a single cost-to-go function to be optimized as shown by:

$$\mathcal{J}(\mathbf{I}_k,\mu_k)=\inf_{\boldsymbol{\theta}_k\in\mathcal{P}_k}\mathrm{Tr}(\mathbf{P}_{k+1|k+1}).\tag{42}$$

In short, the dynamic optimization algorithm encompasses the feedback transmission path, extending from the cost-to-go function computed at the receiver output at the previous cycle to the waveform selection by the transmitter for the next cycle. Most importantly, the whole computation is feasible in an on-line manner by virtue of setting the horizon depth $L=1$.

4.4. Curse of dimensionality

Unfortunately, when we include a horizon depth of L time-steps into the future in the DP algorithm which is a highly desirable thing to do, we run into Bellman's curse-of-dimensionality problem. To explain this important practical issue, we define the following parameters:

- N_z: the measurement-space dimension,
- N_x: the state-space dimension,
- N_g: the waveform-parameter grid size,
- L: dynamic-programming horizon-depth.

In general, the complexity of the dynamic-programming algorithm for waveform selection is on the order of

$$\mathcal{O}\big(N_s^3(2N_z.N_g)^L\big),\tag{43}$$

where $N_s=\max(N_z,N_x)$, the term N_s^3 is for the matrix inversions needed for computation of the expected error covariance matrix, and the term $2N_z$ is for the number of cubature points for computation of the expectation operators for computing the measurements in (41). For this general case, it is assumed that all individual optimizations in each stage of the DP are performed over the complete set of waveform-library grid.

We see from (43) that the main source of complexity in the DP algorithm is attributed to the exponential growth of computations due to the horizon depth L. More specifically, at each stage of depth of DP and for each cubature point in (43) a new search in the waveform library needs to be performed. We refer to such a complete search of the waveform library as the *global search*. As L increases, the level of computation becomes unsustainable.

To mitigate the curse-of-dimensionality problem, we may try to perform the optimization by searching a *local* neighborhood of the current cubature point. In other words, we consider the use of an *explore-exploit strategy* for waveform selection by constraining the DP algorithm to be in a locality of the current cubature point as well as a limited-size neighborhood in the wave-parameter grid. Such a strategy requires the use of memory, which is beyond the scope of FATR.

5. Case study: tracking a falling object in space

5.1. Modeling the scenario of reentry problem

Let us consider an extensively studied problem in the tracking community, i.e. the reentry problem [2]. A ballistic target reenters the Earth's atmosphere after having traveled a long distance, its speed is high and the remaining time to ground impact is relatively short. The goal of a tracking radar, in this case, is to intercept and track a ballistic target shown in Fig. 2. In the reentry phase, two types of forces are in effect. The most dominant is drag, which is a function of speed and has a substantial nonlinear variation in altitude; the second force is due to gravity, which accelerates the target toward the center of the earth. This tracking problem is highly difficult because the target's dynamics change rapidly. Under the influence of drag and gravity acting on the target, the following differential equation governs its motion [2]:

Please cite this article in press as: S. Haykin et al., Control theoretic approach to tracking radar: First step towards cognition, Digital Signal Process. (2011), doi:10.1016/j.dsp.2011.01.004

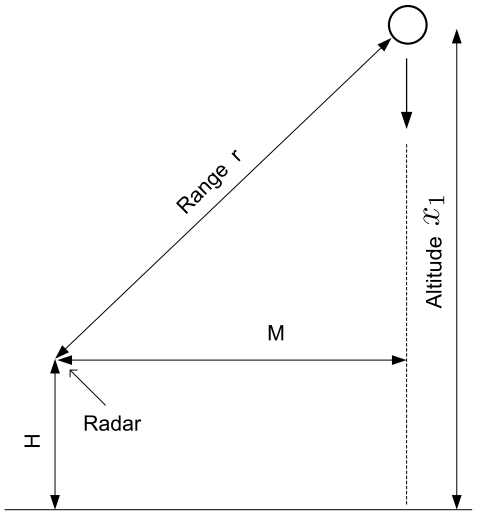

Fig. 2. Geometry of the falling object's scenario.

$$\dot{x}_1 = -x_2,$$
$$\dot{x}_2 = \underbrace{\frac{-\rho(x_1).g.x_2^2}{2x_3}}_{\text{drag}} + g,$$
$$\dot{x_3} = 0, \tag{44}$$

where x_1, x_2 and x_3 are the altitude, velocity and ballistic coefficient that depends on the target's mass, shape, cross-sectional area, and air density, respectively. The term $\rho(x_1)$ is air density and modeled as an exponentially decaying function of x_1, given by

$$\rho(x_1) = \rho_0 \exp(-\gamma x_1),$$

with the proportionality constant $\rho_0 = 1.754$, $\gamma = 1.49 \times 10^{-4}$, and the gravity $g = 9.8\ \text{ms}^{-2}$.

To convert (44) to the state space, we define the state vector as $\mathbf{x} = [x_1\ x_2\ x_3]$. The system equation at continuous time t can now be expressed by

$$\dot{\mathbf{x}}_t = \mathbf{g}(\mathbf{x}_t).$$

Using the Euler approximation with a small integration step δ, we write

$$\mathbf{x}_{k+1} = \mathbf{x}_k + \delta \mathbf{g}(\mathbf{x}_k) = \mathbf{f}(\mathbf{x}_k). \tag{45}$$

In order to account for imperfections in the process model (*e.g.*, lift force, small variations in the ballistic coefficient, and spinning motion), we add zero-mean Gaussian process noise, obtaining the new process equation:

$$\mathbf{x}_{k+1} = \mathbf{f}(\mathbf{x}_k) + \mathbf{v}_k, \tag{46}$$

where we have

$$\mathbf{f}(\mathbf{x}_k) = \Phi \mathbf{x}_k - \mathbf{G}\big[D(\mathbf{x}_k) - g\big] \tag{47}$$

with matrices

$$\Phi = \begin{pmatrix} 1 & -\delta & 0 \\ 0 & 1 & 0 \\ 0 & 0 & 1 \end{pmatrix},$$
$$\mathbf{G} = [0 \quad \delta \quad 0]^T$$

and drag

$$D(\mathbf{x}_k) = \frac{\rho(\mathbf{x}_k[1]) g \mathbf{x}_k^2[2]}{2\mathbf{x}_k[3]}.$$

We assume that the process noise is zero-mean Gaussian with covariance matrix

$$\mathbf{Q} = \begin{pmatrix} q_1 \frac{\delta^3}{3} & q_1 \frac{\delta^2}{2} & 0 \\ q_1 \frac{\delta^2}{2} & q_1 \delta & 0 \\ 0 & 0 & q_2 \delta \end{pmatrix}.$$

The parameters q_1 and q_2 control the amount of process noise in target dynamics and ballistic coefficient, respectively. For our simulation, we consider that $q_1 = 0.01$, $q_2 = 0.01$ and $\delta = 1$.

5.2. Radar configurations

We use LFM with both up-sweep and down-sweep chirps, which composes the waveform library with $\boldsymbol{\Theta} = \{\lambda \in [10e{-}6, 300e{-}6], b \in [-300e8, 300e8]\}$ and grid step-size $\Delta\lambda = 10e{-}6$ and $\Delta b = 50e8$. The bandwidth is set to be 8 MHz. An *X*-band radar fixed at $(0, 0)$ and operated at a fixed carrier frequency of 10.4 GHz with the speed of electromagnetic wave of 3×10^8 m/s is employed in this paper. The length of horizon for the FATR is fixed at two different values $L = 1$ and $L = 2$. The traditional active radar with fixed-waveform is equipped with down-sweep chirp rate and a pulse duration of $\lambda = 20$ μs. The sampling rate is set to $T_s = 100$ ms and the simulations are conducted for 50 Monte Carlo runs. The radar is located at height $H = 30$ m with horizontal distance to the track $M = 30$ km. The measurements at discrete time k include the range r and the range-rate $\dot{r}$, given by

$$r_k = \sqrt{M^2 + \big(\mathbf{x}_k[1] - H\big)^2} + \mathbf{w}_k[1],$$
$$\dot{r}_k = \frac{\mathbf{x}_k[2](\mathbf{x}_k[1] - H)}{\sqrt{M^2 + (\mathbf{x}_k[1] - H)^2}} + \mathbf{w}_k[2],$$

where the measurement noise $\mathbf{w}_k \sim \mathcal{N}(\mathbf{0}, \mathbf{R}_k)$.

Assuming that the transmitter and the receiver are co-located, the received signal energy depends inversely on the fourth power of the target range r. For this reason, the returned pulse SNR η in (9) for the target observed at range r was modeled according to

$$\eta = \left(\frac{r_0}{r}\right)^4,$$

where r_0 was the range at which 0 dB SNR was obtained. For our experiment, r_0 was set to be 50 km.

The true initial state of the target is defined as

$$\mathbf{x}_0 = [61\ \text{km} \quad 3048\ \text{m/s} \quad 19\,161]^T$$

and the initial state estimate and its covariance are assumed to be

$$\hat{\mathbf{x}}_{0|0} = [61.5\ \text{km} \quad 3400\ \text{m/s} \quad 19\,000]^T,$$
$$\mathbf{P}_{0|0} = \text{diag}\big([10^6 \quad 10^4 \quad 10^4]\big).$$

5.3. Performance metric

We use the ensemble-averaged root mean-square error (EA-RMSE) as a metric to evaluate the performance of FATR, compared to a traditional active radar of fixed waveform. The EA-RMSE is defined as

$$\text{RMSE-pos.}(k) = \sqrt{\frac{1}{N}\sum_{n=1}^{N}\big((\epsilon_k^n - \hat{\epsilon}_k^n)^2 + (\eta_k^n - \hat{\eta}_k^n)^2\big)},$$

where (ϵ_k^n, η_k^n) and $(\hat{\epsilon}_k^n, \hat{\eta}_k^n)$ are the true and estimated positions at time index k in the n-th Monte Carlo run. In a similar manner, we may also define the EA-RMSE in velocity.

Please cite this article in press as: S. Haykin et al., Control theoretic approach to tracking radar: First step towards cognition, Digital Signal Process. (2011), doi:10.1016/j.dsp.2011.01.004

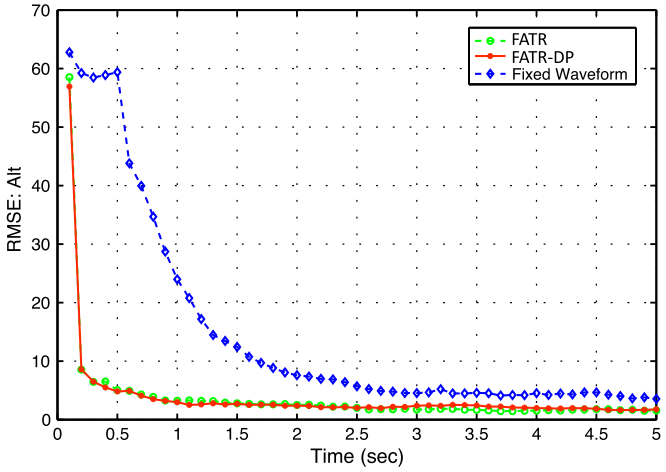

Fig. 3. RMSE of altitude for both fore-active tracking radar (FATR and FATR-DP shown in dotted and solid lines with circle markers) and FWR radar (FWR, shown in dotted line with diamond markers).

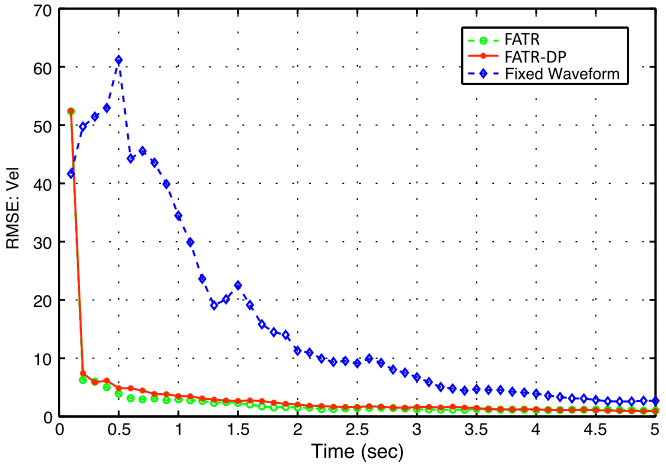

Fig. 4. RMSE of velocity for both fore-active tracking radar (FATR and FATR-DP shown in dotted and solid lines with circle markers) and FWR (FWR, shown in dotted line with diamond markers).

5.4. Simulation results

Here we show the simulations results for both the fore-active tracking radar (FATR) and traditional active radar with fixed-waveform (FWR) that were first reported in Haykin et al. [10]. Figs. 3 and 4 plot the RMSE for altitude and velocity where we see that FATR outperforms a traditional active tracking radar with fixed waveform by an order of magnitude. The results presented in these two figures demonstrate the information processing power of partial cognition facilitated by global feedback. Fig. 5 plots the RMSE for the ballistic coefficient. However, we now see that the use of global feedback does not make a difference to the accuracy of ballistic-coefficient estimation. The reason for lack of improvement in this case is the fact that in our experiment the radar is only equipped with the ability to estimate altitude and velocity. With no provision made for observing the ballistic coefficient, we are in effect confronted with a partially observable problem.

To illustrate how the partial cognition process has evolved in the FATR, we have plotted the waveform selection for both the chirp rate and length of the envelope, shown in Figs. 6 and 7. The transitions of waveform parameters across time explain a *cortex-like behavior* being performed in the FATR.

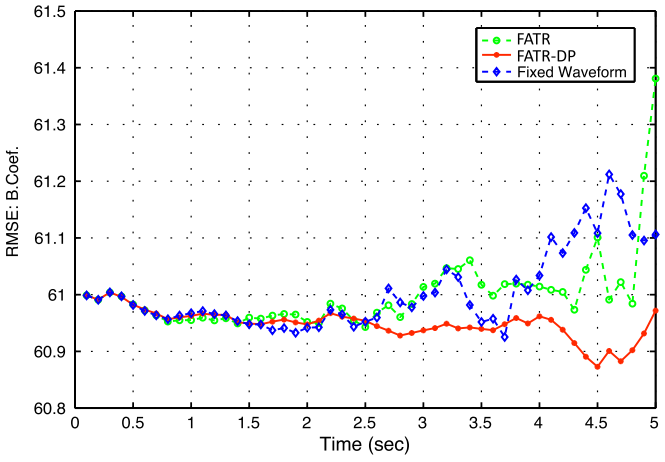

Fig. 5. RMSE of the target ballistic coefficient for both fore-active tracking radar (FATR, and FATR-DP shown in dotted and solid lines with circle markers) and FWR (FWR, shown in dotted line with diamond markers).

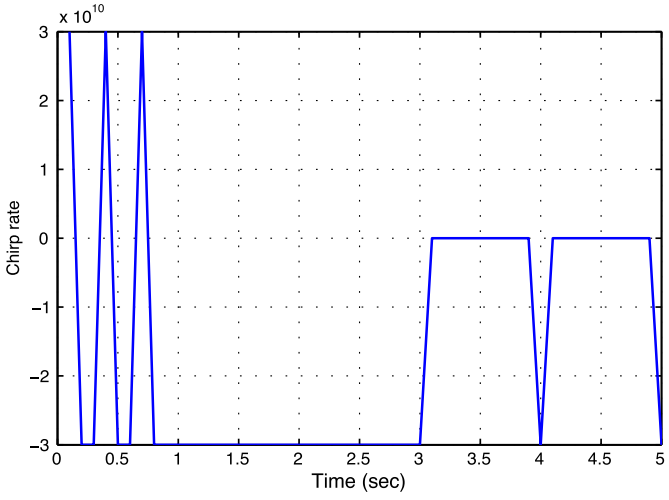

Fig. 6. Waveform selection: the chirp rate.

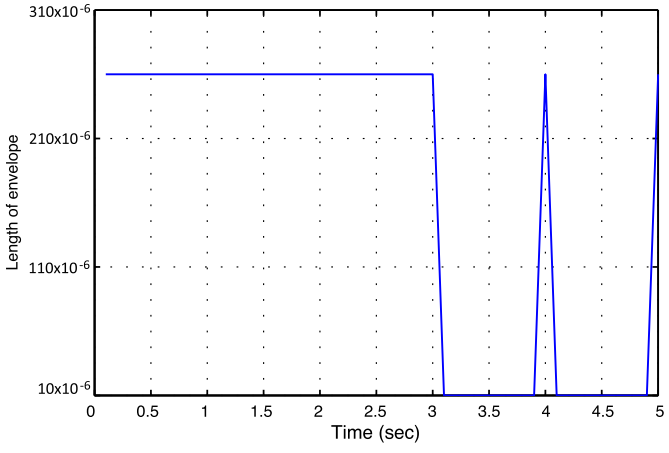

Fig. 7. Waveform selection: the length of envelope.

6. Concluding remarks

In this paper, we have presented the underlying theory of a fore-active (i.e., partially) cognitive tracking radar and used computer simulations to support the theory, demonstrating the ability of this new radar concept to significantly outperform a traditional radar tracker.

Please cite this article in press as: S. Haykin et al., Control theoretic approach to tracking radar: First step towards cognition, Digital Signal Process. (2011), doi:10.1016/j.dsp.2011.01.004

This impressive performance, well illustrated in Figs. 3 and 4, has exploited the following ideas:

(1) Use of the cubature Kalman filter in the receiver for perception of the radar environment; this new filter is the best known approximation to the optimal Bayesian filter under the Gaussian assumption, an assumption that is justified for the tracking of targets in space.
(2) Formulation of a new dynamic-programming algorithm for action to control the waveform selection in the transmitter. This novel algorithm derives its information-processing power in two important ways:
   - First, it is based on the notion of *imperfect-state information*, which gets around the fact that Bellman's dynamic programming requires perfect knowledge of the state, whereas in a real-world radar environment the state is hidden from the observer.
   - Second, clever use is made of the cubature rule of third degree in the approximation of certain integrals involved in deriving the dynamic-programming algorithm.

In sum, focusing solely on the perception-action cycle of cognition, this paper has substantiated the ideas of cognitive radar that were first described in Haykin [8], with the substantiations being done in the context of a tracking radar application.

In the current approach, in the absence of memory thee is no provision within the system to utilize the notion of explore and exploit, i.e. to explore to know where the previous actions are in the landscape of all actions in order to build a local neighborhood of search space for next actions. This has resulted in the agile jumps of the action points in the grid of all possible waveform parameters (e.g. see Figs. 6 and 7). In a forthcoming paper, we will describe the expansion of fore-active radar presented here to a cognitive radar in order to encompass both memory and attention, thereby making the radar all the more powerful.

Acknowledgments

The authors of this paper gratefully acknowledge the financial support provided by the National Science and Engineering Research Council (NSERC) of Canada for work on cognitive radar.

Appendix A. Notations

- b: the chirp rate of the LFM pulse;
- c: speed of the electromagnetic wave propagation;
- $\mathbb{E}[\cdot]$: statistical expectation operator;
- f_c: carrier frequency;
- $f(\cdot)$: system function modeling the state transition;
- $g(\cdot)$: cost function;
- $h(\cdot)$: measurement function modeling the observer;
- $\mathbf{I}_k$: information vector, consisting of the measurements history and waveform history till time k;
- $\mathcal{J}$: cost-to-go function;
- $\mathbf{J}$: Fisher information matrix;
- L: dynamic-programming horizon-depth;
- $n(t)$: Gaussian noise at the radar receiver input, with $\tilde{n}(t)$ denoting its complex envelope;
- N_g: the waveform-parameter grid size;
- N_x: the state-space dimension;
- N_z: the measurement-space dimension;
- $r(t)$: received signal at the receiver input from the target contaminated by Gaussian noise;
- $\mathbf{R}(\boldsymbol{\theta}_{k-1})$: measurement-noise covariance matrix at discrete time k as a function of the transmit waveform parameters $\boldsymbol{\theta}_{k-1}$;
- $\tilde{s}(t)$: complex envelope of the transmitted pulse;
- $s_R(t)$: received signal reflected from the target;
- $s_T(t)$: transmitted radar signal;
- $\mathrm{Tr}(\cdot)$: operator extracting the trace of a matrix;
- $\mathbf{x}_k$: the state vector at time k;
- $\mathbf{z}_k$: the measurement vector at time k;
- $\mathbf{Z}_k \triangleq \{\mathbf{z}_0, \ldots, \mathbf{z}_k\}$: the measurements history;
- ρ: range of the target;
- $\dot{\rho}$: range rate of the target;
- τ: delay between the transmitted and received signal reflected by the target;
- μ: policy function mapping the information vector into an action;
- ν: Doppler shift associated with target radial motion;
- λ: duration of the Gaussian envelope for the linear frequency modulation (LFM) chirp transmit signal;
- $\boldsymbol{\theta}_k = [\lambda_k, b_k]$: the transmit waveform parameters at time k;
- $\boldsymbol{\Theta} k = [\boldsymbol{\theta}_0, \boldsymbol{\theta}_1, \ldots, \boldsymbol{\theta}_k]$: the waveform history;
- η_r: SNR at the reference distance r.

Appendix B. Derivation of the approximation formula in (37)

To the best of our knowledge, the approximation described in (37) appeared for the first time in Kershaw and Evans [13]; Therein, however, no derivation was presented for the approximation. This appendix is intended to fill this gap. For brevity in notation, henceforth, we omit explicit representation of the dependence of $\hat{\mathbf{x}}_{k+1|k+1}$ on $(\mathbf{I}_k, \mathbf{x}_{k+1}, \mathbf{z}_{k+1}, \boldsymbol{\theta}_k)$, that is, we focus on the first line of (34) and thus write

$$g(\mathbf{I}_k, \boldsymbol{\mu}_k) = \mathbb{E}_{\mathbf{x}_{k+1}, \mathbf{z}_{k+1}|\mathbf{I}_k, \boldsymbol{\theta}_k}\big[(\mathbf{x}_{k+1} - \hat{\mathbf{x}}_{k+1|k+1})^T (\mathbf{x}_{k+1} - \hat{\mathbf{x}}_{k+1|k+1})\big] \tag{B.1}$$

$$= \mathbb{E}_{\mathbf{z}_{k+1}|\mathbf{x}_{k+1}, \mathbf{I}_k, \boldsymbol{\theta}_k} \mathbb{E}_{\mathbf{x}_{k+1}|\mathbf{I}_k, \boldsymbol{\theta}_k} \times \big[(\mathbf{x}_{k+1} - \hat{\mathbf{x}}_{k+1|k+1})^T (\mathbf{x}_{k+1} - \hat{\mathbf{x}}_{k+1|k+1})\big] \tag{B.2}$$

where in (B.2), we used the definition of conditional expectation.

The expectation in (B.2) is over the distribution $p(\mathbf{z}_{k+1}|\mathbf{x}_{k+1}, \mathbf{I}_k, \boldsymbol{\theta}_k)$. Observer that within the measurement prediction and update cycles of the CKF discussed in Section 3, the measurements are functions of $\boldsymbol{\theta}_k$ solely through the noise covariance $\mathbf{R}(\boldsymbol{\theta}_k)$ defined in (12). Recognizing that the parameter vector $\boldsymbol{\theta}_k$ is irrelevant once the measurement $\mathbf{z}_k$ is available to the receiver, we are justified to approximate the distribution $p(\mathbf{z}_{k+1}|\mathbf{x}_{k+1}, \mathbf{I}_k, \boldsymbol{\theta}_k)$ by the predicted measurement distribution $p(\mathbf{z}_{k+1}|\mathbf{I}_k, \boldsymbol{\theta}_k)$. In other words, we may set $\mathbb{E}_{\mathbf{z}_{k+1}|\mathbf{x}_{k+1}, \mathbf{I}_k, \boldsymbol{\theta}_k}(\cdot) \approx \mathbb{E}_{\mathbf{z}_{k+1}|\mathbf{I}_k, \boldsymbol{\theta}_k}(\cdot)$, we may therefore write

$$\begin{aligned} g(\mathbf{I}_k, \boldsymbol{\mu}_k) &\approx \mathbb{E}_{\mathbf{z}_{k+1}|\mathbf{x}_{k+1}, \mathbf{I}_k, \boldsymbol{\theta}_k} \mathbb{E}_{\mathbf{x}_{k+1}|\mathbf{I}_k, \boldsymbol{\theta}_k} \times \big[(\mathbf{x}_{k+1} - \hat{\mathbf{x}}_{k+1|k+1})^T (\mathbf{x}_{k+1} - \hat{\mathbf{x}}_{k+1|k+1})\big] \\ &= \mathbb{E}_{\mathbf{z}_{k+1}|\mathbf{I}_k, \boldsymbol{\theta}_k} \mathbb{E}_{\mathbf{x}_{k+1}|\mathbf{I}_k, \boldsymbol{\theta}_k}\big[(\mathbf{x}_{k+1} - \hat{\mathbf{x}}_{k+1|k+1})^T (\mathbf{x}_{k+1} - \hat{\mathbf{x}}_{k+1|k+1})\big] \\ &= \mathbb{E}_{\mathbf{z}_{k+1}|\mathbf{I}_k, \boldsymbol{\theta}_k}\big[\mathbb{E}_{\mathbf{x}_{k+1}|\mathbf{I}_k, \boldsymbol{\theta}_k}\big[(\mathbf{x}_{k+1} - \hat{\mathbf{x}}_{k+1|k+1})^T (\mathbf{x}_{k+1} - \hat{\mathbf{x}}_{k+1|k+1})\big]\big]. \end{aligned} \tag{B.3}$$

Next, using the identity $\mathbf{x}^T\mathbf{y} = \mathrm{Tr}(\mathbf{y}\mathbf{x}^T)$ and the fact that order of the expectation and the trace are interchangeable, we may go on to write

$$\begin{aligned} g(\mathbf{I}_k, \boldsymbol{\mu}_k) &\approx \mathbb{E}_{\mathbf{z}_{k+1}|\mathbf{I}_k, \boldsymbol{\theta}_k}\big[\mathbb{E}_{\mathbf{x}_{k+1}|\mathbf{I}_k, \boldsymbol{\theta}_k}\big[(\mathbf{x}_{k+1} - \hat{\mathbf{x}}_{k+1|k+1})^T (\mathbf{x}_{k+1} - \hat{\mathbf{x}}_{k+1|k+1})\big]\big] \\ &= \mathbb{E}_{\mathbf{z}_{k+1}|\mathbf{I}_k, \boldsymbol{\theta}_k}\big[\mathrm{Tr}\big(\mathbb{E}_{\mathbf{x}_{k+1}|\mathbf{I}_k, \boldsymbol{\theta}_k} \times \big[(\mathbf{x}_{k+1} - \hat{\mathbf{x}}_{k+1|k+1})(\mathbf{x}_{k+1} - \hat{\mathbf{x}}_{k+1|k+1})^T\big]\big)\big]. \end{aligned} \tag{B.4}$$

Please cite this article in press as: S. Haykin et al., Control theoretic approach to tracking radar: First step towards cognition, Digital Signal Process. (2011), doi:10.1016/j.dsp.2011.01.004

By definition, the expression of $\mathrm{Tr}(\cdot)$ in (B.4) is the state-estimation error covariance $\mathbf{P}_{k+1|k+1}$; hence,

$$g(\mathbf{I}_k, \boldsymbol{\mu}_k) \approx \mathbb{E}_{\mathbf{z}_{k+1}|\mathbf{I}_k,\theta_k}\left[\mathrm{Tr}(\mathbf{P}_{k+1|k+1})\right]. \tag{B.5}$$

Finally nothing that in the CKF, $\mathbf{P}_{k+1|k+1}$ is independent of the measurement $\mathbf{z}_{k+1}$, we have arrived at the desired approximation

$$g(\mathbf{I}_k, \boldsymbol{\mu}_k) \approx \mathbb{E}_{\mathbf{z}_{k+1}|\mathbf{I}_k,\theta_k}\left[\mathrm{Tr}(\mathbf{P}_{k+1|k+1})\right] = \mathrm{Tr}(\mathbf{P}_{k+1|k+1}). \tag{B.6}$$

References

[1] I. Arasaratnam, S. Haykin, Cubature Kalman filters, IEEE Trans. Automat. Control 54 (6) (2009).
[2] M. Athans, R.P. Wishner, A. Bertolini, Suboptimal state estimation for continuous-time nonlinear systems from discrete noise measurements, IEEE Trans. Automat. Control 13 (1968) 504–514.
[3] R. Bellman, Dynamic Programming, Princeton University Press, Princeton, NJ, 1957.
[4] D.P. Bertsekas, Dynamic Programming and Optimal Control, vol. 1, 3rd ed., Athena Scientific, Belmont, MA, 2005, pp. 217–279.
[5] R. Cools, Computing cubature formulas: the science behind the art, Acta Numer. 6 (1997) 1–54.
[6] J.M. Fuster, Cortex and Mind, Oxford University Press, 2003.
[7] S. Haykin, Communication Systems, 4th ed., Wiley, 2000.
[8] S. Haykin, Cognitive radar: a way of the future, IEEE Signal Process. Magaz. 23 (2006) 30–40.
[9] S. Haykin, Keynote lecture on cognitive dynamic systems, NIPS 2009, Whistler, BC, Canada, http://soma.mcmaster.ca, 2009.
[10] S. Haykin, A. Zia, Y. Xue, I. Arasaratnam, Cognitive tracking radar. Provisional patent, No. 1022P001US01, 2009.
[11] S. Haykin, Cognitive Dynamic Systems, Cambridge University Press, 2011.
[12] Y.C. Ho, R.C.K. Lee, A Bayesian approach to problems in stochastic estimation and control, IEEE Trans. Automat. Control 9 (1964) 333–339.
[13] D.J. Kershaw, R.J. Evans, Optimal waveform selection for tracking systems, IEEE Trans. Inform. Theory 40 (1994) 1536–1550.
[14] D.J. Kershaw, R.J. Evans, Waveform selective probabilistic data association, IEEE Trans. Aerospace Electron. Syst. 33 (1997) 1180–1188.
[15] H.L. Van Trees, Detection, Estimation and Modulation Theory, Part III, Wiley, New York, 1971, pp. 294–297, 338.
[16] P. Woodward, Probability and Information Theory, with Applications to Radar, Pergamon, New York, 1953.

Simon Haykin received the B.Sc. (first-class honors), Ph.D., and D.Sc. degrees, all in Electrical Engineering from the University of Birmingham, England.

Currently, he is the University Professor at McMaster University, Hamilton, ON, Canada. He is a pioneer in adaptive signal-processing with emphasis on applications in radar and communications, an area of research which has occupied much of his professional life. In the mid-1980s, he shifted the thrust of his research effort in the direction of Neural Computation, which was reemerging at that time. All along, he had the vision of revisiting the fields of radar and communications from a brand new perspective. That vision became a reality in the early years of this century with the publication of two seminal journal papers: (i) "Cognitive Radio: Brain-Empowered Wireless Communications," IEEE J. Selected Areas in Communications, Feb. 2005, (ii) "Cognitive Radar: A Way of the Future," IEEE J. Signal Processing, Feb. 2006. Cognitive radio and cognitive radar are two important parts of a much wider and multidisciplinary subject: cognitive dynamic systems, research into which has become his passion.

Prof. S. Haykin is a Fellow of the Royal Society of Canada. He is the recipient of the Henry Booker Medal of 2002, the Honorary Degree of Doctor of Technical Sciences from ETH Zentrum, Zurich, Switzerland, in 1999, and many other medals and prizes.

Amin Zia received his Ph.D. in Electrical and Computer Engineering from McMaster University, Hamilton, Ontario, Canada in 2007. He is currently a research fellow at the Department of Cell and Systems Biology at the University of Toronto, Ontario, Canada, where he is conducting research on the applications of statistical signal processing and information theory in computational biology. Amin's current interests include statistical signal processing, information theory and computational biology.

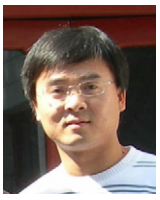

Yanbo Xue received his B.Sc. degree in Automation Engineering, M.A.Sc. degree in Control Theory and Engineering from Northeastern University, China in 2001 and 2004, and Ph.D. degree in Electrical and Computer Engineering from McMaster University, Hamilton, Ontario, Canada in 2010, respectively. His Ph.D. dissertation titled 'Cognitive Radar: Theory and Simulations' was the first doctoral thesis on cognitive radar. He is currently working as a research fellow at the Cognitive Systems Laboratory of McMaster University. Yanbo's current research interests include cognitive dynamic systems with emphasis on cognitive radar, target detection and tracking, neural networks and learning machines, control theory, and array signal processing.

Ienkaran Arasaratnam received the B.Sc. degree (first-class honors) in Electronics and Telecommunication Engineering from the University of Moratuwa, Sri Lanka in 2003 and the M.A.Sc. and Ph.D. degrees in Electrical and Computer Engineering from McMaster University, Hamilton, ON, Canada in 2006 and 2009, respectively. For his Ph.D. dissertation titled "Cubature Kalman Filtering: Theory and Applications," he formulated a new approximate nonlinear Bayesian filter called the "Cubature Kalman Filter." He is currently working as a R&D engineer at Ford motor company of Canada Ltd. His main research interests include signal processing, control and machine learning with applications to target tracking and fault diagnosis in conventional and electric powertrains. Many of his research work can be found at his website https://sites.google.com/site/haranarasaratnam/.

Dr. Arasaratnam received the Mahapola Merit Scholarship during his undergraduate studies. He is the recipient of the Outstanding Thesis Research Award at M.A.Sc. Level in 2006, the Ontario Graduate Scholarship in Science and Technology in 2008 and NSERC's Industrial Research & Development Fellowship in 2010.

Please cite this article in press as: S. Haykin et al., Control theoretic approach to tracking radar: First step towards cognition, Digital Signal Process. (2011), doi:10.1016/j.dsp.2011.01.004